

Yield stress and elastic modulus of suspensions of noncolloidal particles in yield stress fluids

Fabien Mahaut, Xavier Chateau, Philippe Coussot, Guillaume Ovarlez*[†]

Université Paris Est - Institut Navier

Laboratoire des Matériaux et Structures du Génie Civil (UMR 113 LCPC-ENPC-CNRS)

2, allée Kepler, 77420 Champs-sur-Marne, France

May 6, 2019

Synopsis

We study experimentally the behavior of isotropic suspensions of noncolloidal particles in yield stress fluids. This problem has been poorly studied in the literature, and only on specific materials. In this paper, we manage to develop procedures and materials that allow focusing on the purely mechanical contribution of the particles to the yield stress fluid behavior, independently of the physicochemical properties of the materials. This allows us to relate the macroscopic properties of these suspensions to the mechanical properties of the yield stress fluid and the particle volume fraction, and to provide results applicable to any noncolloidal particle in any yield stress fluid. We find that the elastic modulus/concentration relationship follows a Krieger-Dougherty law, and show that the yield stress/concentration relationship is related to the elastic modulus/concentration relationship through a very simple law, in agreement with results from a micromechanical analysis.

*corresponding author: guillaume.ovarlez@lcpc.fr

[†]Support from the Agence Nationale de la Recherche (ANR) is acknowledged (grant ANR-05-JCJC-0214).

I Introduction

Dense suspensions arising in industrial processes (concrete casting, drilling muds, foodstuff transport...) and natural phenomena (debris-flows, lava flows...) often involve a broad range of particle sizes. The behavior of these materials reveal many complex features which are far from being understood (for a recent review, see Stickel and Powell (2005)). This complexity originates from the great variety of interactions between the particles (colloidal, hydrodynamic, frictional, collisional...) and of physical properties of the particles (volume fraction, deformability, sensitivity to thermal agitation, shape, buoyancy...) involved in the material behavior.

Basically, these materials exhibit a yield stress and have a solid viscoelastic behavior below this yield stress; above the yield stress they behave as liquids, and their flow behavior is usually well fitted to a Herschel-Bulkley law [Larson (1999)] although the exact details of the constitutive law seem more complex at the approach of the transition between the liquid and the solid regimes [Coussot (2005)]. The yielding behavior originates from the colloidal interactions which create a jammed network of interacting particles [Larson (1999); Coussot (2005)]. If the behavior of dense colloidal suspensions, and more generally of yield stress fluids, have received considerable interest and been widely studied, the influence of the large particles on this behavior have been poorly studied. Moreover, the few existing experimental studies have focused on very specific material e.g. particles in a clay dispersion [Coussot (1997), Ancy and Jorrot (2001)], a cement paste [Geiker *et al.* (2002)], a foam [Cohen-Addad *et al.* (2007)] or coal slurries [Sengun and Probst (1989a,b)]. This poses a problem: can we use the results obtained in studies performed with noncolloidal particles in clay dispersions to predict the behavior of a mortar (i.e. particles in a cement paste)? In other words, how far can these studies be used to predict the behavior of any kind of noncolloidal particles suspended into any kind of yield stress fluid? Let us review some of the results obtained in the literature regarding the viscoelastic properties, the yield stress, and the flow properties, in order to specify this problem.

As yield stress fluids are viscoelastic solids under the yield stress, it is worth looking at the

problem of particles in viscoelastic materials. The influence of particles on the linear viscoelastic properties of materials have been a little more studied (see e.g. Poslinski *et al.* (1988); See *et al.* (2000); Walberer and McHugh (2001)) than their influence on yield stress fluids as they are of great importance for the design of composite material and filled polymers. However, it is difficult to infer a general result from these studies: e.g. See *et al.* (2000) find that 40% of spherical 80 μm polyethylene particles increase the elasticity of a silicon oil and a Separan polymer solution by a factor 5, whereas they find that 40% of spherical 60 μm polyethylene particles increase the elasticity of the same matrixes by a factor 8; on the other hand, Poslinski *et al.* (1988) find that 40% of 15 μm glass beads increase the elasticity of thermoplastic polymers by a factor 15. Therefore, one may still wonder what is the influence of the exact physicochemical origin of the viscoelasticity of the material on the suspension mechanical properties, and if there are specific physicochemical interactions between the large particles and the matrix in the various studies quoted above.

Only a few studies deal with the influence of the noncolloidal particles on the suspending fluid yield stress [Coussot (1997), Ancy and Jorrot (2001), Geiker *et al.* (2002)]. Moreover, these studies provide extremely different results; e.g., when spherical particles are embedded at a volume fraction corresponding to 70% of the maximum packing fraction in a cement paste, Geiker *et al.* (2002) find that the yield stress of the paste is increased by a factor 50, whereas Ancy and Jorrot (2001) find that when they are embedded in a clay dispersion the yield stress is increased only by a factor 2. (Note however that such discrepancy may find its origin in the yield stress measurement method as Geiker *et al.* (2002) use a Herschel-Bulkley fit of the flow curve, and Chateau *et al.* (2007) have shown that such a fit provides an overestimation of the yield stress of the suspension). Moreover, Ancy and Jorrot (2001) found in some cases that the suspension yield stress can be lower than the suspending paste yield stress; as pointed out by Chateau *et al.* (2007), this should not occur if the noncolloidal particle interact only mechanically with the paste. As a consequence, Ancy and Jorrot (2001) propose an interpretation based on

a local depletion of the colloidal particles near the large particles. These results are therefore unlikely to apply if the same particles are embedded in another paste: the experimental results and their theoretical interpretation do not depend only on the suspending paste yield stress but also on the composition of the suspending paste and cannot be applied if e.g. the suspending paste is not a colloidal suspension.

Sengun and Probstein (1989a,b) have investigated the flow properties of suspensions of large particles in a colloidal suspension: they have studied experimentally bimodal coal slurries, and have provided a general model to predict the viscosity of such suspensions. Their model relates the shear-rate dependent viscosity of the material to the large particle volume fraction and the fine particles suspension rheological properties, independently of their exact composition. Such a model should therefore apply to suspensions of any large particles in any non-Newtonian fluid; however, unfortunately, Sengun and Probstein (1989a,b) did not perform experiments for non-Newtonian suspending fluids of other microscopic composition than coal slurries. Moreover, they did not study the problem of the influence of the large particles on the yield stress. Note that a critical review of existing theories aiming at describing the influence of noncolloidal particles in non-Newtonian fluids can be found in Chateau *et al.* (2007).

As a consequence of these results, it is of high importance to clarify the cases where the mechanical properties of the suspension depend only on the mechanical properties of the suspending fluid and on the large particle volume fraction and size distribution; this should provide results applicable to any particles in any yield stress fluid. Any departure from the generic results would then be the result of specific physicochemical interactions (or specific slippage at the paste/particle interface) and would justify a specific study with the particular particles and particular paste involved. With the aim of providing such generic results, we perform an experimental study on a broad range of materials.

In this study, we focus on the case where scale separation is possible between the paste microstructure (i.e. the colloidal particle size in the case of dense suspensions) and the noncol-

loidal particles in suspension. Then, a simplification occurs: these materials can be considered in a first step as noncolloidal particles embedded in a paste (e.g. fresh concrete \approx sand and granulate + cement paste; debris-flows \approx rocks + mud). Therefore, we will consider the paste as a continuum medium, of known mechanical properties, in which the noncolloidal particles are embedded. Moreover, we do not want to study a specific case (e.g. gravel in cement) but we want to understand what happens in the general case of any rigid noncolloidal particles embedded in any yield stress fluid, i.e. we focus on the purely mechanical contribution of the particles to the paste behavior, independently of the physicochemical properties of the materials. In order to achieve this goal, we must check several things: (i) that the particle size is much larger than the paste microstructure size, (ii) that the results depend only on the mechanical properties of the paste i.e. that they are independent of the physicochemical origin of the yield stress, (iii) that the results are independent of the noncolloidal particles size (when the particles are monodisperse), (iv) that there are neither particle/particle nor particle/paste physicochemical interactions.

Finally, the problem we deal with is the homogenization of a suspension of isotropically distributed monodisperse rigid spheres dispersed in a continuum yield stress fluid. The present paper is devoted to the experimental realization of this problem, while Chateau *et al.* (2007) deal with the theoretical problem. Here, we focus on the behavior of the pastes in their solid regime, i.e. on the influence of the particles on the elastic modulus and the yield stress.

In Sec. II, we present the materials employed and the experimental setup. We present the elastic modulus measurements in Sec. III, and the yield stress measurements in Sec. IV. We finally show in Sec. V that the yield stress/concentration relationship is related to the elastic modulus/concentration relationship through a very simple law, in agreement with recent results from a micromechanical analysis presented in a companion paper [Chateau *et al.* (2007)].

II Materials and methods

The materials and procedures presented hereafter are designed to fulfill the requirements for studying the purely mechanical contribution of an isotropic distribution of rigid monodisperse particles to the yield stress fluids behavior.

A Pastes and particles

As a suspending paste, we use various pastes: an emulsion, a physical gel, and a colloidal suspension.

The emulsion is a water in oil emulsion. As the continuous phase, we use a dodecane oil in which a Span 80 emulsifier is dispersed at a 7% concentration. A 300g/l CaCl_2 solution is dispersed in the oil phase at 6000rpm during 1 hour. In the emulsion the origin of the yield stress and elasticity is the surface tension between the droplets [Larson (1999)]. The microstructure scale is thus given by the droplets which have a size of order $1\mu\text{m}$ from microscope observations. The yield stress can be varied by varying the droplet concentration: we vary the droplet concentration between 70 and 90%, and obtain 5 materials of yield stress between 6 and 100Pa.

The physical gel is Carbopol dispersion. Here we use a Carbopol 980 (from Noveon) dispersed in water at a 0.7% concentration, that provides a Carbopol gel of 100Pa yield stress. The Carbopol is dispersed at 1000rpm during 30min, then neutralized with NaOH at pH=7. The gel is then stirred during an entire day to ensure homogeneity of the material. The exact structure of Carbopol gels is poorly known, and it depends a lot on the Carbopol used. Basically, the polymers arrange in roughly spherical blobs which tend to swell in water [Ketz *et al.* (1988); Carnali and Naser (1992)]; above a sufficient concentration, the blobs are squeezed together and the material develops a yield stress. The microstructure size of these materials is badly known; from Cryo-SEM experiments [Kim *et al.* (2003)] one sees that it may be as low as a few micrometers; microrheological measurements by Oppong *et al.* (2006) also indicate that it

is larger than $1\mu\text{m}$. However, a modelling of their behavior gives an indirect indication that the blobs may have a typical size of $100\mu\text{m}$ (it actually depends on pH). We tried to observe the microstructure of the Carbopol gel with an environmental SEM, but we failed to see anything; that is why, in order to ensure scale separation between the particles and the gel, we used particles as large as 2mm in the case of Carbopol gels.

The colloidal suspension is a bentonite suspension; it is made of (smectite) clay particles of length of order $1\mu\text{m}$ and thickness 10nm. Water molecules tend to penetrate between the elementary layers composing each particle which thus swell; the particles are then squeezed together but also interact through electrostatic forces; it results in a yield stress. The yield stress can be varied by varying the particle concentration: we vary the concentration between 3 and 9%, and obtain 6 materials of initial yield stress between 6 and 150Pa. Note that we give the 'initial' value of the yield stress (i.e. 100s after a preshear at high shear rate) as these suspensions are thixotropic: their yield stress (and elastic modulus) increases with the rest time.

Finally, we have prepared materials with 3 kinds of yield stress physicochemical origins (jammed elastic blobs, surface tension, colloidal interactions). If we obtain the same behavior when adding solid particles in the 3 materials, this ensures that there is no contribution from specific particles/material physicochemical interactions. Another important test arises from the bentonite suspension, which is thixotropic: if the yield stress evolution kinetics remains unchanged when adding the particles, then it is another indication that there are no physicochemical interactions between the particles and the material.

The particles are spherical monodisperse beads. We use either polystyrene beads of density 1.05, or glass beads of density 2.5. This allows to check that there are neither beads/beads nor beads/paste interactions: no difference should result in the measurements performed with different particles unless there are interactions specific to the materials used. Note in particular that the polystyrene beads are hydrophobic whereas the glass beads are hydrophilic: this detail may be important when the particles are embedded in the emulsion as the hydrophobic parti-

cles are then preferably surrounded by the continuous phase (the oil) whereas the hydrophilic particles are preferably surrounded by the dispersed phase (the water). We test various particle diameters: 80, 140, 315 μm in the case of the polystyrene beads, and 140, 330 and 2000 μm in the case of the glass beads.

In the bentonite suspension and emulsion cases, the bead size is much larger than the paste microstructure; in the case of the Carbopol gel, it is undoubtedly true for the mm beads only and the comparison of the results between the μm and mm bead will give an indication of the relevant microstructure scale: the results should be independent of the bead size unless this size is as low as the microstructure scale.

We study suspensions of noncolloidal particles in yield stress fluids at a volume fraction ϕ ranging between 0 and 50%. When preparing a suspension of beads in a yield stress fluid, the insertion of air is unavoidable. However, methods such as centrifugation to remove the bubbles cannot be used if we want to ensure that the materials remain homogeneous and isotropic as explained in Sec. IIB. It is therefore important to check that the air content is negligible. E.g., with PS particles larger than 250 μm in a bentonite suspension, we observed that for more than 30% of beads the air content was of the order of 5% of the material; this did not occur with glass beads: the air is more likely to be entrained by the hydrophobic (PS) particles in a suspension. It has to be noted that the effect of air is not negligible: it changes not only the continuous phase mechanical properties [Larson (1999)] but also the effective bead volume fraction, which is a sensitive parameter at high volume fractions. As an example, a 40% suspension of 315 μm PS beads in a bentonite suspension yields an elastic modulus 30% lower than a 40% suspension of 330 μm glass beads in the same bentonite suspension, because of a 6% air content in the case of the PS beads. We chose to work with a constant volume of material in order to check that the air content is always lower than 1%. All the measurements we present in this paper were performed on materials with as negligible an air content. We chose not to study volume fractions higher than 50% because we failed to prepare reproducible materials at such high volume fractions,

probably because of the unavoidable presence of air in the materials in these cases.

Finally, note that the beads need to be carefully washed in order to avoid surface interactions due to remaining surfactant/stabilizer at the surface of the polystyrene beads following their production process. The beads are washed in an ultrasound bath during 30 minutes and then dried. We observed that when the unwashed beads are embedded into a Carbopol gel, it actually results in a lower yield stress than when the washed beads are suspended, indicating residual surface effects. A single washing is enough to ensure a reproducible state.

Note however that despite all the precautions we took, we will show in the Appendix A that the particles may still induce non mechanical effects that we do not understand; however, we will present in this Appendix A a method to eliminate unambiguously from the analysis materials in which physicochemical interactions between the particles and paste may have occurred.

B Rheological methods

Most rheometric experiments are performed within a vane in cup geometry (inner radius $R_i = 12.5\text{mm}$, outer cylinder radius $R_e = 18\text{mm}$, height $H = 45\text{mm}$) on a commercial rheometer (Bohlin C-VOR 200) that imposes either the torque or the rotational velocity (with a torque feedback). In order to avoid wall slip [Coussot (2005)], we use a six-blade vane as an inner tool, and we glue sandpaper of roughness equivalent to the size of the particles on the outer cylinder wall. For the 2mm particles, we use another six-blade vane in cup geometry (inner radius $R_i = 22.5\text{mm}$, outer cylinder radius $R_e = 45\text{mm}$, height $H = 45\text{mm}$). Working within these wide-gap geometries allows to study easily large particles and to ensure that for all the materials studied, there are enough particles in the gap to consider that we measure the properties of a continuum medium (the suspension).

We measure the elastic modulus $G'(\phi)$ and yield stress $\tau_c(\phi)$ of the paste as a function of the volume fraction ϕ of large particles embedded in the pastes. As long as we work in the linear regime of the materials, the stress inhomogeneities in the wide gap geometry do not

affect the elastic modulus measurements, e.g. for an elastic deformation resulting in an angular displacement θ of the inner tool and a torque T , the elastic modulus G' can be computed as $\frac{T}{4\pi H\theta}(\frac{1}{R_i^2} - \frac{1}{R_e^2})$. On the other hand, the shear stress τ continuously decreases within the gap: the shear stress at a radius R is $\tau(R) = \frac{T}{2\pi HR^2}$. Therefore, one has to choose a definition of the shear stress that is measured in a given rheological experiment. Here, we want to perform yield stress measurements; whatever the measurement method we choose, yield first occurs where the stress is maximal i.e. along the inner virtual cylinder. As consequence, we define the shear stress measurement as $\tau(R_i) = \frac{T}{2\pi HR_i^2}$, so that the yield stress τ_c is correctly measured (any other definition would provide an underestimation). Anyway, we will focus on the evolution of the dimensionless elastic modulus $G'(\phi)/G'(0)$ and the dimensionless yield stress $\tau_c(\phi)/\tau_c(0)$ with the bead volume fraction ϕ , which should be independent of a particular definition of τ .

Elastic modulus measurement method

The elastic modulus G' is determined through oscillatory shear experiments in the linear regime: in most experiments, an oscillatory shear stress of amplitude τ_0 is applied at a frequency of 1Hz. As we work with a controlled stress rheometer, an oscillatory shear stress is imposed rather than an oscillatory shear strain, in order to get accurately small deformations. The amplitude τ_0 depends on the sample: it is chosen so as to ensure that the strain induced on the tested material is lower than 10^{-3} , so that all materials are tested in their linear regime. These experiments were performed with several different amplitudes on some materials in order to check the independence of the results on the choice of τ_0 (see Sec. III, Fig. 5a). We also checked the independence of the results on the frequency (see Sec. III, Fig. 5b): even if the elastic modulus $G'(0)$ of the paste may depend on the frequency, the dimensionless modulus $G'(\phi)/G'(0)$ should not depend on it.

In Fig. 1, we present elastic modulus measurements performed on the 3 pastes. We observe that the elastic modulus of the bentonite suspension strongly increases with the time of rest

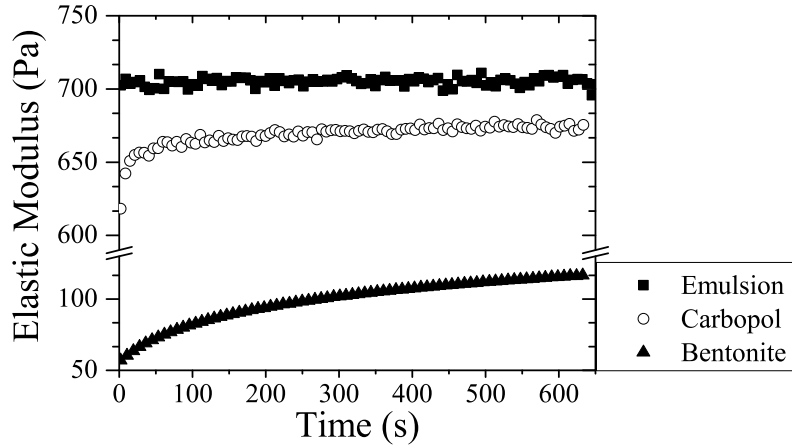


Figure 1: Elastic modulus G' vs. time after loading when an oscillatory shear stress of amplitude $\tau_0 = 0.3\text{Pa}$ is applied at a frequency of 1Hz to an emulsion (squares), a Carbopol gel (open circles), and $\tau_0 = 0.1\text{Pa}$ at 1Hz to a bentonite suspension (triangles).

(by a factor 2 in 5 minutes); this is characteristic of the aging at rest of thixotropic materials [Coussot *et al.* (2006)]. On the other hand, the emulsion elastic modulus is constant within 0.5% and the Carbopol gel elastic modulus increases only slightly (5% during 10 minutes).

Yield stress measurement method

Performing a yield stress measurement is still challenging [Coussot (2005)], and there are a lot of methods designed to evaluate this yield stress; several were used recently by Uhlerr *et al.* (2005) on various yield stress fluids. These methods may give different results if e.g. the material ages with the time of rest [Cheng (1986)]. In this case the yield stress at which a flow stops (the dynamic yield stress) differs for the yield stress at which the flow starts (the static yield stress), and the later is a function of the time of rest in the solid state. The static yield stress can be measured through the vane method [Nguyen and Boger (1985); Liddell and Boger (1996)]: in this method the vane tool is driven at a low velocity, and the yield stress for a given time of rest is defined by the overshoot presented by the shear stress (if the material is thixotropic) in a shear stress vs. strain plot, or by the shear stress plateau if it is not thixotropic. The static

yield stress can also be measured by means of the simple inclined plane test [Coussot and Boyer (1995)], by measuring the angle between a plane and the horizontal for which a given layer of material starts to flow along this plane under the effect of gravity; the inclined plane can also be used to measure the dynamic yield stress by measuring the thickness of a material when its flow stops for a given angle of the plane. This last property can also be measured through the slump test [Pashias *et al.* (1996); Roussel and Coussot (2005)], or through creep tests [Coussot *et al.* (2006)]: if a creep stress above the yield stress is imposed then the material flows steadily whereas for a creep stress below the yield stress there is a creep flow that is slowing down at any time and the strain tends to saturate. A simple way to evaluate both the static yield stress and the dynamic yield stress is to impose increasing and decreasing shear stress ramps [Uhlerr *et al.* (2005)], or increasing and decreasing shear rate ramps.

A question is now: are all these methods relevant in the case of suspensions of noncolloidal particles in yield stress fluids? In order to illustrate the problems that appear when trying to perform a yield stress measurement on these materials, we present an example of ascending/descending shear rate sweeps in Fig. 2 for a pure emulsion, and for the same emulsion filled with 20% of $140\mu\text{m}$ PS beads. In these experiments, constant shear rates increasing from 0.01 to 10s^{-1} and then decreasing from 10 to 0.01s^{-1} were applied during 30s, and the stationary shear stress was measured for each shear rate value.

As the emulsion is not thixotropic, we observe the same curve for the ascending/descending shear rate sweeps, and the low shear rate value provides a good evaluation of the yield stress value (here 90Pa). We would expect to find the same independence when the emulsion is filled with particles. Surprisingly, we find that the shear stress during the ascending shear rate sweep differs from the shear stress during the descending shear rate sweep. From Fig. 2, the static yield stress would then be 110Pa whereas the dynamic yield stress would be 90Pa as in the pure emulsion. However, we find that any measurement performed after this experiment gives a static yield stress equal to the stopping yield stress, i.e. 90Pa. Therefore, there have been

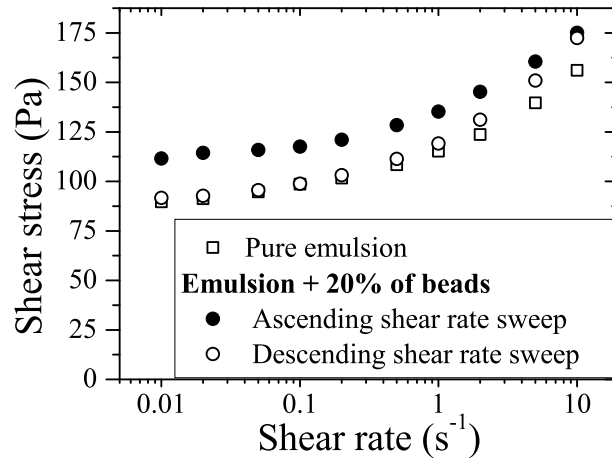


Figure 2: Shear stress vs. shear-rate for ascending/descending shear rate sweeps in a pure emulsion (open squares) and for the same emulsion filled with 20% of $140\mu\text{m}$ PS beads (filled/open circles).

some irreversible change. This irreversible change is probably particle migration towards the low shear zones; this phenomenon is well documented in the case of suspensions in Newtonian fluids [Leighton and Acrivos (1987b); Abbott *et al.* (1991); Graham *et al.* (1991); Phillips *et al.* (1992); Nott and Brady (1994); Mills and Snabre (1995); Morris and Boulay (1999); Shapley *et al.* (2004); Ovarlez *et al.* (2006)] but is still badly known in yield stress fluids (some studies exist however in viscoelastic fluids [Tehrani (1996); Huang and Joseph (2000); Lormand and Phillips (2004)]). An indication that there is indeed migration is given by the experiments performed on suspensions of particles in a Carbopol gel: as the Carbopol gel is transparent, we have been able to observe qualitatively the particle distribution, and we observed that there seems to remain not a single particle near the vane tool after shearing the material. On the other hand, at low shear rate in a Couette geometry the flow of yield stress fluids is localized near the inner tool [Coussot (2005)] because the shear stress decreases continuously from the inner radius to the outer radius and is then lower than the yield stress only in a fraction of the gap near the outer cylinder. As a consequence, at low shear rate during the descending shear rate sweep, only the pure emulsion is flowing and contributes to the shear stress as there are no more particles near

the inner tool: this explains why the same apparent value of the yield stress is found in the suspension during the descending sweep as in the pure emulsion with this method; on the other hand, the yield stress at the beginning of the very first ascending sweep is that of the suspension as migration has not occurred yet.

This implies that we cannot use a method based on a shear flow such as creep tests and shear rate ramps, and that we cannot preshear our materials. Note that this casts doubt on the measurements performed e.g. by Coussot (1997) and Geiker *et al.* (2002): their yield stress measurement is the low shear rate limit of a flow curve; we can legitimately wonder if their results are really characteristic of the materials at the mean volume fraction. On the other hand, the use of the slump test by Ancey and Jorrot (2001) is likely to provide a fair evaluation of the yield stress as the slump flow may have induced only a small deformation.

That is why for the yield stress measurements we chose to perform a single measurement at a constant velocity on each sample, without any initial preshear. Fig. 3 shows the shear stress vs. strain for yield stress measurement experiments performed in a bentonite suspension, an emulsion and a Carbopol gel.

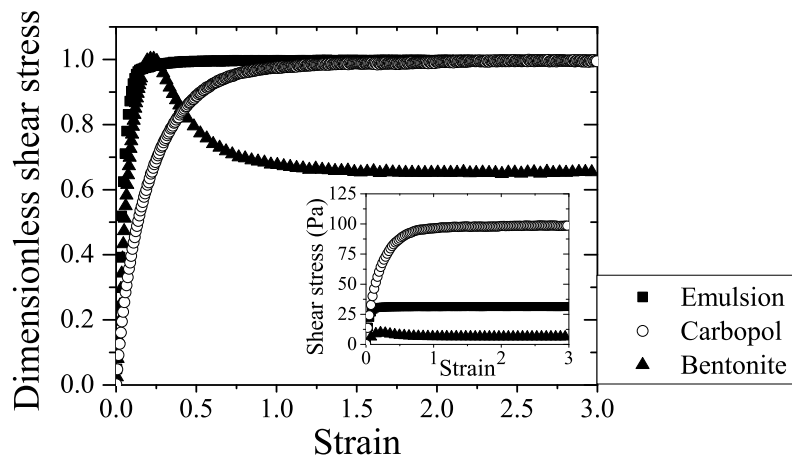


Figure 3: Dimensionless shear stress vs. strain when slowly shearing a material from rest at $10^{-2} s^{-1}$, after a 600s rest time: emulsion (squares), Carbopol gel (empty circles), and bentonite suspension (triangles); the shear stress is divided by the defined yield stress. Inset: stress vs. strain for the same experiments.

In all cases there is first a linear increase of stress with strain: this corresponds to the elastic deformation of the materials. In the case of the emulsion and the Carbopol gel, there is then a plateau, corresponding to the plastic flow at low shear rate: this defines the yield stress of these materials. In the case of the bentonite suspension, there is an overshoot, followed by a slow decrease of the shear stress: the peak defines the yield stress, the decrease corresponds to destructuration of the material under the shear flow. Note that in the case of the bentonite suspension and the emulsion, the maximum (or the plateau) is reached for a strain of order 0.2, whereas in the case of the Carbopol gel one has to wait for a strain of order 1. In this later case, it is thus likely that the particle distribution starts to be anisotropic at the yield point (see e.g. Gadala-Maria and Acrivos (1980); Parsi and Gadala-Maria (1987) for the case of particles in a Newtonian fluid); we will comment on this point hereafter.

Summary of the procedure

Finally the procedure is the following:

- a suspension of beads in a yield stress fluid is prepared at a given volume fraction ϕ of beads ranging between 0 and 50% in the cylinder. There is no preshear after preparation; however, in order to perform all the measurements in the same conditions in the case of thixotropic materials (see the bentonite suspension data in Fig.1), i.e. to start from a same state of destructuration of the material with and without particles, it is necessary to strongly stir the material by hand after loading. This procedure allows to avoid shear induced migration, and importantly also to perform measurements on an isotropic microstructure that allows for comparison with micromechanical models [Chateau *et al.* (2007)]: any controlled shear of the material would induce an anisotropic microstructure as observed in suspensions of particles in Newtonian fluids [Gadala-Maria and Acrivos (1980); Parsi and Gadala-Maria (1987); Morris and Brady (1996); Sierou and Brady (2002)].
- then, the vane tool is slowly inserted and oscillations are performed at rest in the linear

regime during 10 minutes in order to get the elastic modulus; note that it is important to measure the elastic modulus evolution in time (and not its mean value) even for non thixotropic materials: this allows evidencing undesirable physicochemical interactions between the particles and the paste with some materials as we will show in the Appendix A.

- afterwards, a small rotational velocity is imposed to the vane tool in order to get the yield stress; we checked that the elasticity measurement is nonperturbative: the same yield stress is measured if a zero stress is imposed instead of oscillations before the yield stress measurement.

Finally, as the yield stress measurement may induce migration and a microstructure anisotropy, any new measurement requires a new sample preparation. Note that the manual preparation does not strictly ensure that we always get the same initial state of destructuration in the case of thixotropic materials; that is why the yield stress measurement is performed after 10 minutes of rest: any slight initial irreproducibility have a negligible influence on the structure after such a time of rest.

Consequences of the absence of a controlled preshear

Usually, before any measurement on a material, a preshear is applied in order to ensure a reproducible state. In our experiments, we could not preshear the material by rotating the inner tool at a high velocity: we showed that in order to avoid shear induced migration and to ensure an isotropic distribution of the particles, it is important to stir the material by hand without favoring any direction of shear. It is now important to evaluate how reproducible our preparation is, and what the absence of a controlled preshear implies on the materials behavior.

Let us see what happens in the case of the Carbopol gel. In Fig. 4a we show the yield stress measurements performed on the pure Carbopol gel in 3 different experiments:

- in a first experiment, we preshear the material by rotating the inner cylinder at high velocity (corresponding to a shear rate of 10s^{-1}) during 60s, and then we measure the

yield stress by imposing a slow velocity (corresponding to a shear rate of 0.01s^{-1}) in the same direction as the preshear after a 600s rest

- in a second experiment, we preshear the material by rotating the inner cylinder at high velocity (corresponding to a shear rate of 10s^{-1}) during 60s, and then we measure the yield stress by imposing a slow velocity (corresponding to a shear rate of 0.01s^{-1}) in the opposite direction to the preshear after a 600s rest
- in a third experiment, we preshear the material by hand during 60s and then we measure the yield stress by imposing a slow velocity (corresponding to a shear rate of 0.01s^{-1}) after a 600s rest

The role of the 600s rest before the yield stress measurement is to erase all possible thixotropic effects.

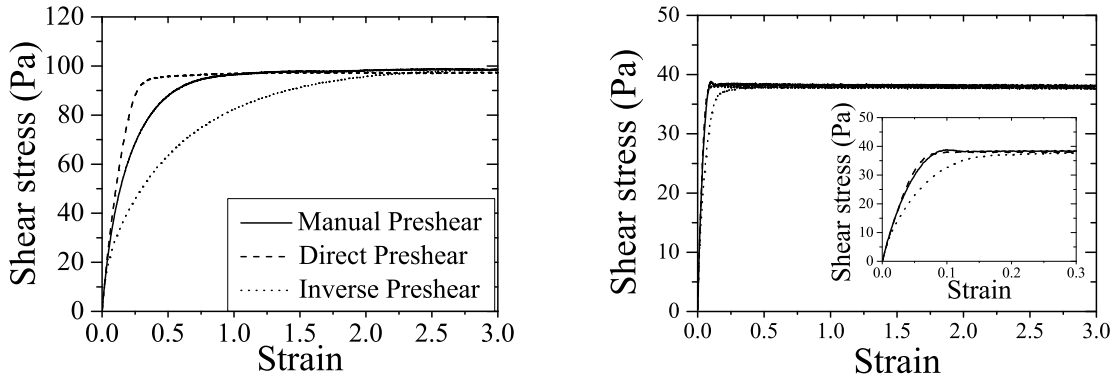


Figure 4: a) Stress vs. strain when slowly shearing a pure Carbopol gel from rest at 10^{-2}s^{-1} , after a 600s rest time, in three situations: when a 60s preshear at 10s^{-1} is first applied in the same direction as the yield stress measurement (dashed line); when a 60s preshear at 10s^{-1} is first applied in the opposite direction to the yield stress measurement (dotted line); when a 60s random manual preshear is first performed (solid line). b) Same figure in the case of an emulsion; the inset is a zoom of Fig. 4b

We observe that in the three cases, the same plateau is reached. However the critical strain for reaching this plateau varies between 0.2 when the yield stress measurement is performed in

the same direction as the preshear, to 2 when the preshear is performed in the opposite direction to the yield stress measurement. This shows actually that the Carbopol gel gets structured by the shear (note that this is not a reversible thixotropic effect as the same state would be recovered after a 600s rest in this later case). It is also possible to show that in the case where the direction of the preshear is opposite to the direction of the yield stress measurement, when the stress is unloaded from any stress before the plateau, the material does not go back to its initial state but is irreversibly deformed; this irreversible deformation corresponds to the progressive structural change of the material (it is likely that the polymer chains are progressively oriented by the shear).

Once the material is structured, the low shear rate plateau is reached and is the same for all initial conditions: this means that the same anisotropic state of the paste is reached, and, importantly, that the yield stress measurement is not affected by the preshear: whatever the reproducibility of our manual preshear, we thus expect to get a fair evaluation of the yield stress.

If a random manual preshear is applied to the material, the stress/strain curve falls somewhere between the two other curves and the plateau is reached for a strain of about 1. A consequence is that the elasticity measurement is affected: we found that the elastic modulus measurement is reproducible within 0.5% when a preshear is applied with the rheometer, whereas the manual preshear results in a reproducibility of the elastic modulus of about 5%: this explains partly the scatter of data in Sec. III. Moreover, as mentioned above (and as will be shown at the end of Sec. IV), in the case of a manual preshear, the yield stress measurement is performed for a strain sufficient for the particle distribution to be anisotropic when the yield stress measurement is performed.

This would mean that the elastic measurement and the yield stress measurement may not be performed exactly on the same structure of the suspension for two reasons: (i) the interstitial Carbopol gel is not structured the same way at rest when the elasticity measurement is performed and at the shear stress plateau where the yield stress is measured; (ii) the particle distribution

is isotropic for the elasticity measurement, and is possibly slightly anisotropic for the yield stress measurement. Point (i) is actually of no importance as far as we deal with dimensionless quantities: as long as the interstitial paste is of a single kind for all the elasticity measurements, and of a single kind for all the yield stress measurements, whatever the volume fraction is, the effect of the particles on both the dimensionless elastic modulus and the dimensionless yield stress will be fairly evaluated. Point (ii) is actually more of an issue and difficult to check: a strain of order 1 is sufficient to induce a significant anisotropy [Gadala-Maria and Acrivos (1980)], and it may produce an additional scatter when the yield stress data obtained on all materials are plotted.

Finally, note that these features were also observed in the emulsion but the phenomenon is less pronounced and the critical strain at the yield point is at the maximum of order 0.2 i.e. the point (ii) raised above (anisotropy of particles at the yield point) is probably of no importance in this case. In the case of moderately dense bentonite suspensions, there was not such complexity as the material was initially fluid (fully destructured). However, it is important to note that this complexity exists as Carbopol gels are often used as a model yield stress fluids. It seems here that they are not that model, and that much care should be taken with these materials; another problem with these materials when dealing with particles of different sizes is presented in the Appendix A, .

III Elastic modulus

In this section, we summarize the results of the elastic modulus measurements performed on all the materials. The elastic modulus G' is measured with the method presented in Sec. II B. We study the evolution of the dimensionless modulus $G'(\phi)/G'(0)$ with the volume fraction ϕ of noncolloidal particles for all the materials studied.

Influence of the experimental parameters

In Fig. 5, we plot the dimensionless elastic modulus $G'(\phi)/G'(0)$ vs. the beads volume fraction ϕ for measurements performed at various frequencies and amplitudes on a suspension of $140\mu\text{m}$ polystyrene beads in a bentonite suspension. We observe that the evolution of the dimensionless elastic modulus with ϕ is independent of the frequency and the amplitude as long as we are in the linear regime: this measurement method thus provides a fair evaluation of the influence of the inclusion of rigid particles on the elasticity of a yield stress fluid. We also checked that the dimensionless elastic modulus of a suspension of $140\mu\text{m}$ polystyrene beads in an emulsion is independent of the frequency and the stress amplitude. In all the other experiments presented hereafter, all the results were obtained at a frequency of 1Hz and a given stress amplitude (dependent on the material studied) in the linear regime.

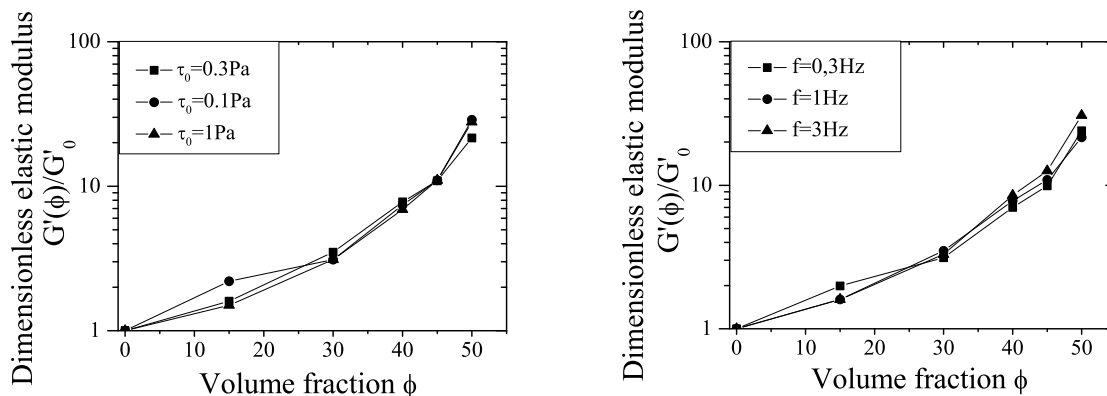


Figure 5: Dimensionless elastic modulus $G'(\phi)/G'(0)$ vs. bead volume fraction ϕ for a suspension of $140\mu\text{m}$ polystyrene beads in a bentonite suspension. The dynamic measurements were performed at a frequency of 1Hz with a stress amplitude $\tau_0 = 0.1, 0.3,$ and 1Pa (left figure), and also at a frequency $f=0.3, 1,$ and 3Hz with a stress amplitude of 0.3Pa (right figure).

Structuration kinetics

In Fig. 6a, we plot the evolution with the rest time t of the elastic modulus $G'(\phi, t)$ of suspensions of $140\mu\text{m}$ polystyrene beads in a bentonite suspension for a volume fraction of beads ϕ ranging

between 0 and 50%. We plot the dimensionless elastic modulus $G'(\phi, t)/G'(0, t)$ as a function of time for the same materials in Fig. 6b.

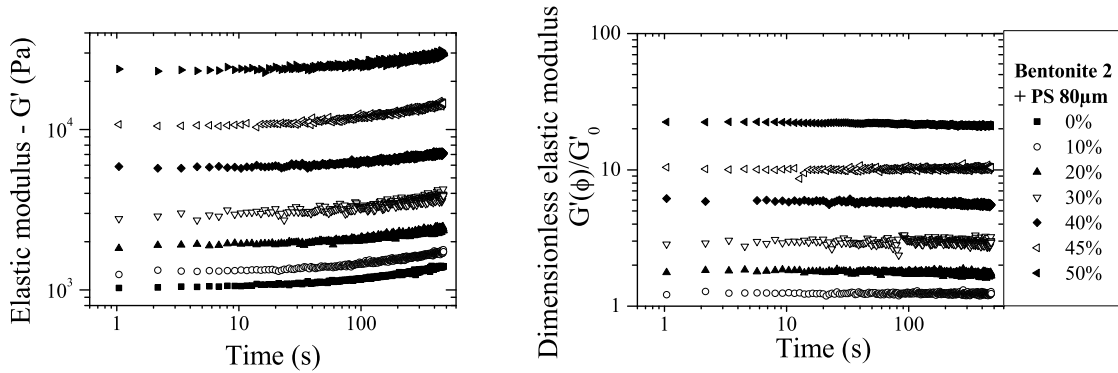


Figure 6: a) Elastic modulus $G'(\phi, t)$ vs. rest time for suspensions of $80\mu\text{m}$ polystyrene beads in a bentonite suspension, for bead volume fraction ϕ ranging between 0 and 50% (see legend). b) Dimensionless elastic modulus $G'(\phi, t)/G'(0, t)$ vs. rest time for the same materials.

We observe in Fig. 6a that the elastic modulus is an increasing function of the time of rest whatever the bead volume fraction; this evolution is due to the bentonite suspension structuration at rest. We also observe in Fig. 6b that the dimensionless elastic modulus $G'(\phi, t)/G'(0, t)$ is independent of time. This means that the effect of time and of the volume fraction can be separated, i.e. the elastic modulus of the suspension at volume fraction ϕ can be written as $G'(\phi, t) = G'(0, t)f(\phi)$. In other words, this means that the structuration kinetics of the bentonite suspension is not affected by the presence of beads: this is consistent with our aim that there should be no physicochemical interactions between particles and paste. Finally, the function $f(\phi)$ is what we are seeking i.e. the function accounting for the mechanical strengthening of the material due to the presence of rigid inclusions.

We show in the Appendix A that even in the case of non (or slightly) thixotropic materials, it is worth measuring the elastic modulus evolution in time with and without particles: it is a powerful mean for evidencing specific physicochemical interactions between the particles and some materials.

Influence of the materials, the bead size and the paste elastic modulus (and yield stress) value

In Fig. 7, we plot the dimensionless elastic modulus $G'(\phi)/G'(0)$ vs. the beads volume fraction ϕ for suspensions of 140 μm polystyrene and glass beads in two different bentonite suspensions, and various emulsions of elastic modulus varying between 300Pa and 3000Pa. We observe that the evolution of the dimensionless elastic modulus is independent of the material, i.e. it is independent of the physicochemical origin of the material elasticity and the bead material; this shows that there are probably no physicochemical interactions between the particles and the pastes. Moreover, we observe that, as expected, the results are independent of the paste elastic modulus, i.e. the elastic modulus of the suspension at volume fraction ϕ can be written as $G'(\phi) = G'(0)f(\phi)$.

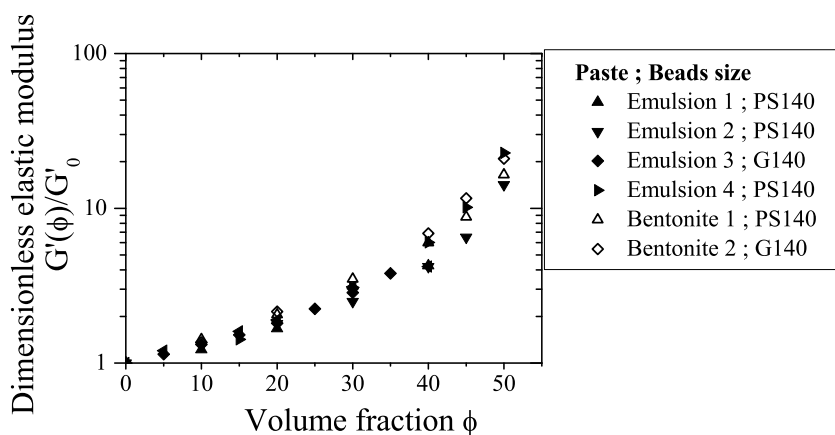


Figure 7: Dimensionless elastic modulus $G'(\phi)/G'(0)$ vs. the beads volume fraction ϕ for a suspension of 140 μm polystyrene (PS) and glass (G) beads in 2 different bentonite suspensions and 4 different emulsions (of elastic modulus varying between 300Pa and 3000Pa).

In Fig. 8, we plot the dimensionless elastic modulus $G'(\phi)/G'(0)$ vs. the beads volume fraction ϕ for suspensions of beads of various sizes in a bentonite suspension. We observe that the evolution of the dimensionless elastic modulus is independent of the bead size (and of the bead material, see Fig. 7); this is consistent with the absence of physicochemical interactions between the particles and between the particles and the pastes.

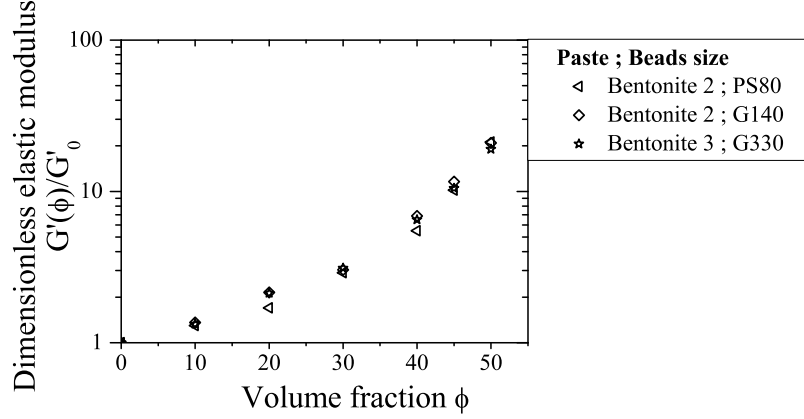


Figure 8: Dimensionless elastic modulus $G'(\phi)/G'(0)$ vs. the beads volume fraction ϕ for suspensions of 80, 140, and 330 μm beads in a bentonite suspension.

Summary of the results on all materials

In Fig. 9, we plot a summary of all the dimensionless elastic modulus measurements $G'(\phi)/G'(0)$.

In Tab.1 we summarize the mean elastic modulus values measured on all the materials (when several measurements were performed at a given concentration), their standard deviation, and the number of materials on which these values were obtained.

Concentration (%)	Mean Dimensionless Elastic Modulus	Standard Deviation (%)	Number of materials
10	1.30	5.4	9
15	1.55	4.6	6
20	1.90	9.3	9
30	2.96	11	13
40	5.62	17	12
45	9.42	23	11
50	18.9	14	10

Table 1: Mean elastic modulus values and standard deviation (in %) as a function of the particle volume fraction.

We observe that we have managed to obtain the purely mechanical contribution of the

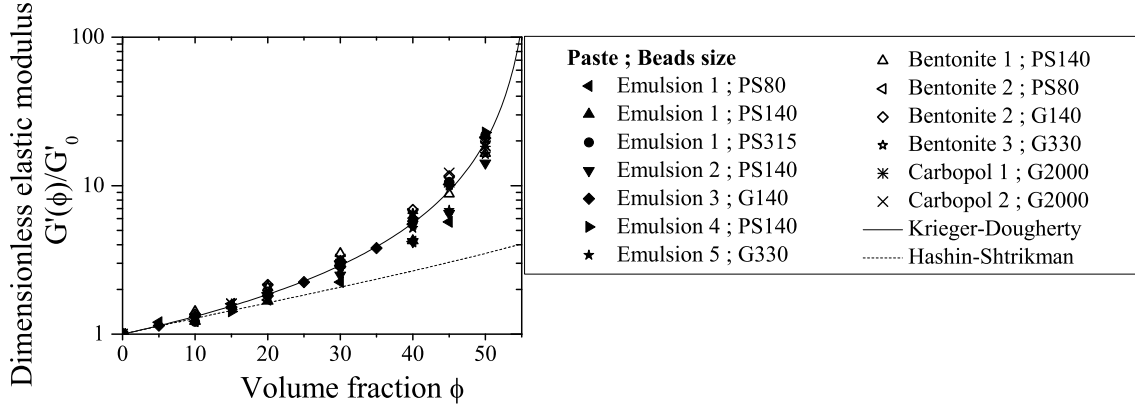


Figure 9: Dimensionless elastic modulus $G'(\phi)/G'(0)$ vs. the beads volume fraction ϕ for suspensions of 80, 140, and 315 μm polystyrene beads (PS) and 140 μm , 330 μm and 2mm glass beads (G) in various bentonite suspensions, emulsions and Carbopol gels. The solid line is a Krieger-Dougherty law $(1 - \phi/\phi_m)^{-2.5\phi_m}$ with $\phi_m = 0.57$. The dotted line is the Hashin-Shtrikman bound $(2 + 3\phi)/(2 - 2\phi)$.

particles to the paste behavior, independently of the physicochemical properties of the materials, i.e. the strengthening of the materials is given by a function $f(\phi)$ of the volume fraction ϕ only: the elastic modulus of an isotropic suspension of monodisperse noncolloidal spherical rigid particles of any size (larger than the yield stress fluid microstructure) embedded at a volume fraction ϕ in a yield stress fluid of elastic modulus $G'(0)$ (that may be a function of time) can be written as $G'(\phi) = G'(0)f(\phi)$. Consistently, we note that the data points all fall above the Hashin-Shtrikman lower bound [Hashin and Shtrikman (1963)]

$$\frac{G'(\phi)}{G'(0)} > \frac{2 + 3\phi}{2 - 2\phi} \quad (1)$$

which is a theoretical bound computed in the more general case of a biphasic material (an infinitely rigid phase embedded in a linear elastic phase) isotropic both at the microscopic and the macroscopic scales, with no physicochemical interactions. Note finally that the consistency between all results, as well as their perfect agreement with the Einstein law $G'(\phi)/G'(0) = 1 + 2.5\phi$ at low volume fraction, show that there is no slippage at the paste/bead interface

during the elastic modulus measurement (in the case of full slippage, the exact result in the dilute limit would be $G'(\phi)/G'(0) = 1 + \phi$ [Larson (1999)]).

The effect of the particle concentration on the elastic modulus is rather important, even for low bead volume fraction: we find $G'(\phi) \approx 1.9 \times G'(0)$ for $\phi = 20\%$ and $G'(\phi) \approx 18 \times G'(0)$ for $\phi = 50\%$. Note that the scatter of data is much higher than what can be found (by the same experimentalist i.e. with exactly the same methods) when measuring the viscosity of suspensions of noncolloidal particles suspended in various Newtonian fluids (see e.g. Fig. 9 in Zarraga *et al.* (2000)): this is expected as flow properties correspond to a mean over all the configurations explored during flow, whereas the static properties are measured over a particular configuration. Moreover, we have shown in Sec. II that the necessary absence of a controlled preshear is an important source of scatter. Finally, as mentioned in Sec. IIA, we control the air content only up to 1%; this induces a 1% uncertainty on the bead volume fraction. For a 50% beads volume fraction, from Eq. 2, this yields a 10% uncertainty on the elastic modulus.

We observe that our data are very well fitted to a Krieger-Dougherty law [Krieger and Dougherty (1959)]

$$G'(\phi) = G'(0) \frac{1}{(1 - \phi/\phi_m)^{2.5\phi_m}} \quad (2)$$

We find $\phi_m = 0.57$ with a least-squares fit of all the experimental data. The Krieger-Dougherty law is usually found to fit most viscosity data of suspension of noncolloidal particles in Newtonian fluids. Therefore, the good agreement with our data is not surprising as the problem of the elasticity of a suspension of rigid particles in a linear elastic material is formally similar to the problem of the viscosity a suspension of rigid particles in a Newtonian (thus linear) material. Note however that the $\phi_m = 0.57$ value we find is lower than the 0.63 value often found for the viscosity of suspensions [Larson (1999)] and than the 0.605 measured locally recently by

Ovarlez *et al.* (2006) through MRI techniques. This discrepancy is likely due to the fact that most experiments in the literature on the viscosity of suspensions are performed on an anisotropic microstructure induced by the flow [Parsi and Gadala-Maria (1987)], whereas our experiments are performed on an isotropic microstructure.

IV Yield stress

In this section, we summarize the results of the yield stress measurements performed on all the materials. The yield stress τ_c is measured with the method presented in Sec. IIB. We study the evolution of the dimensionless yield stress $\tau_c(\phi)/\tau_c(0)$ with the volume fraction ϕ of noncolloidal particles for all the materials studied.

Influence of the experimental parameters

In Fig. 10, we plot the dimensionless yield stress $\tau_c(\phi)/\tau_c(0)$ vs. the beads volume fraction ϕ for measurements performed at two different shear rates on suspensions of $140\mu\text{m}$ polystyrene beads in an emulsion. Importantly, we observe that even if the absolute value of the yield stress may depend on the shear rate (and more generally on the yield stress measurement method) the evolution of the dimensionless yield stress with the volume fraction is independent of the shear rate (as long as it is low enough): while there is a 10% difference between yield stresses measured at 0.01 and 0.003 s^{-1} , the dimensionless stresses values are equal within less than 1%. Therefore, this measurement method provides a fair evaluation of the influence of the inclusion of rigid particles on the resistance of a yield stress fluid. In all the experiments presented hereafter, all the results were obtained at a shear rate $\dot{\gamma} = 0.01\text{ s}^{-1}$.

Summary of the results on all materials

In the case of the yield stress measurements, we showed the same features as for the elastic modulus measurements, i.e. all the results are consistent with our aim that there should be no

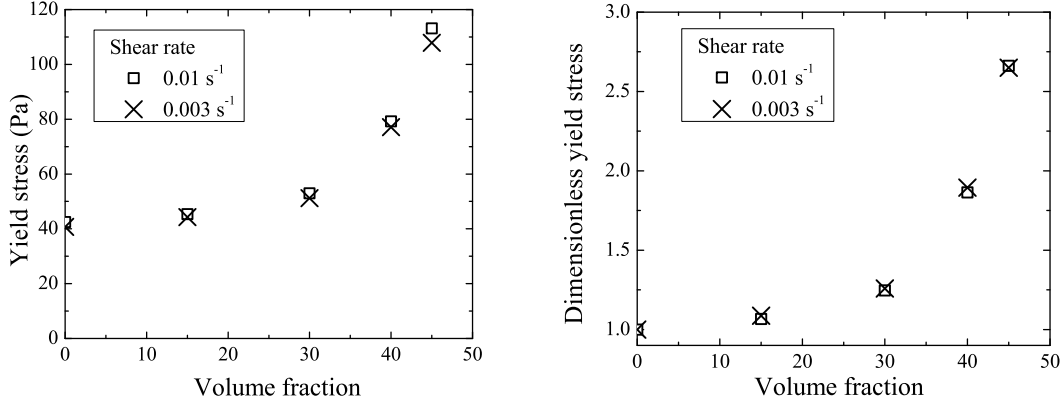


Figure 10: Yield stress $\tau_c(\phi)$ (left) and dimensionless yield stress $\tau_c(\phi)/\tau_c(0)$ (right) vs. the beads volume fraction ϕ for a suspension of $140\mu\text{m}$ polystyrene beads in an emulsion. The yield stress measurements were performed at shear rates $\dot{\gamma} = 0.003\text{s}^{-1}$ (crosses) and 0.01s^{-1} (empty squares).

physicochemical interactions between the particles and the pastes:

- the dimensionless yield stress $\tau_c(\phi, t)/\tau_c(0, t)$ for suspensions in a thixotropic material (the bentonite suspension) is independent of time, i.e. the yield stress of the suspension at volume fraction ϕ can be written as $\tau_c(\phi, t) = \tau_c(0, t)g(\phi)$. This shows again that the structuration kinetics of the bentonite suspension is not affected by the presence of beads.
- the dimensionless yield stress $\tau_c(\phi)/\tau_c(0)$ is independent of the physicochemical origin of the material yield stress, of the bead material and of the bead size.
- the dimensionless yield stress $\tau_c(\phi)/\tau_c(0)$ is independent of the paste yield stress.

In Fig. 11, we plot a summary of the dimensionless yield stress measurements $\tau_c(\phi)/\tau_c(0)$ performed on all the materials. In Tab.2 we summarize the mean yield stress values measured on all the materials (when several measurements were performed at a given concentration), their standard deviation, and the number of materials on which these values were obtained.

We observe that we have managed to obtain the purely mechanical contribution of the particles to the paste behavior, independently of the physicochemical properties of the materials,

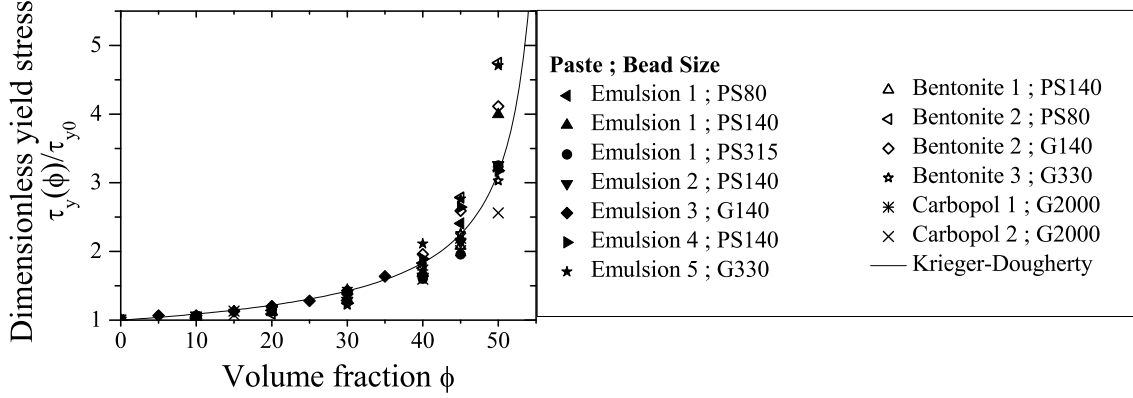


Figure 11: Dimensionless yield stress $\tau_c(\phi)/\tau_c(0)$ vs. the beads volume fraction ϕ for suspensions of 80, 140, and 315 μm polystyrene beads (PS) and 140 μm , 330 μm and 2mm glass beads (G) in various bentonite suspensions, emulsions and Carbopol gels. The solid line is a law $\sqrt{(1 - \phi) \times (1 - \phi/\phi_m)^{-2.5\phi_m}}$ with $\phi_m = 0.57$.

Concentration (%)	Mean dimensionless yield stress	Standard Deviation (%)	Number of materials
10	1.05	1.5	9
15	1.12	2.5	4
20	1.15	3.1	9
30	1.32	5.4	12
40	1.76	9.2	12
45	2.35	13	11
50	3.57	20	11

Table 2: Mean yield stress values and standard deviation (in %) as a function of the particle volume fraction.

i.e. the strengthening of the materials is given by a function $g(\phi)$ of the volume fraction ϕ only: the yield stress of a suspension of monodisperse noncolloidal spherical rigid particle of any size (larger than the yield stress fluid microstructure) embedded at a volume fraction ϕ in a yield stress fluid of yield stress $\tau_c(0)$ (that may depend on time) can be written as $\tau_c(\phi) = \tau_c(0)g(\phi)$. As in the case of the elastic modulus measurements, we observe a good consistency between all results, which means that there is no (or negligible) slippage at the paste/bead interface during the yield stress measurement.

We note that the function $g(\phi)$ is different from the function $f(\phi)$ obtained for the dimensionless elastic modulus measurement: the effect of the volume fraction of noncolloidal particles on the yield stress is actually much less important than its effect on the elastic modulus. The yield stress $\tau_c(\phi)$ at a volume fraction $\phi = 30\%$ is only 40% higher than the yield stress $\tau_c(0)$ of the yield stress fluid, whereas its elasticity $G'(\phi)$ is almost 200% higher than the yield stress fluid elasticity $G'(0)$; for $\phi = 50\%$, $\tau_c(\phi) \approx 3.2 \times \tau_c(0)$ while $G'(\phi) \approx 18 \times G'(0)$. This is very different from the behavior of colloidal suspension: their yield stress follows roughly the same evolution as their elastic modulus with the volume fraction ψ of colloidal particles (see Appendix B for an example). Finally, note that the scatter of the yield stress values is of the order of the scatter observed in the elastic modulus measurements.

The data are well fitted to a law

$$\frac{\tau_c(\phi)}{\tau_c(0)} = \sqrt{\frac{1 - \phi}{(1 - \phi/\phi_m)^{2.5\phi_m}}} \quad (3)$$

with $\phi_m = 0.57$ (see Fig. 11); we will provide a justification for this law in Sec. V.

Finally, our observation that the yield stress of suspensions of noncolloidal particles embedded in a thixotropic paste of time-dependent yield stress $\tau_c(0, t)$ reads $\tau_c(\phi, t) = \tau_c(0, t)g(\phi)$ has an interesting consequence for materials formulation. This means that it is sufficient to know how the interstitial paste evolves to predict the suspension evolution at rest. This may be of

importance for materials like concretes as their behavior is hard to measure: a good knowledge of the cement paste structuration at rest is sufficient.

The yield stress measurement: a destructive measurement

In order to evidence the change of the material due to the yield stress measurement, we have performed a second elasticity measurement just after the yield stress measurement on some pastes. In Fig. 12 we plot the evolution with the bead volume fraction ϕ of the dimensionless elastic modulus $G'(\phi)/G'(0)$ measured before and after the yield stress measurement in suspensions of 2mm glass beads in a Carbopol gel, both measurements ($G'(\phi)$ and $G'(0)$) being performed in the same conditions (i.e. both before or both after the yield stress measurement). In all the yield stress measurement experiments, the inner tool was driven at a velocity of $0.01s^{-1}$ during 300s, resulting in a strain value of 3.

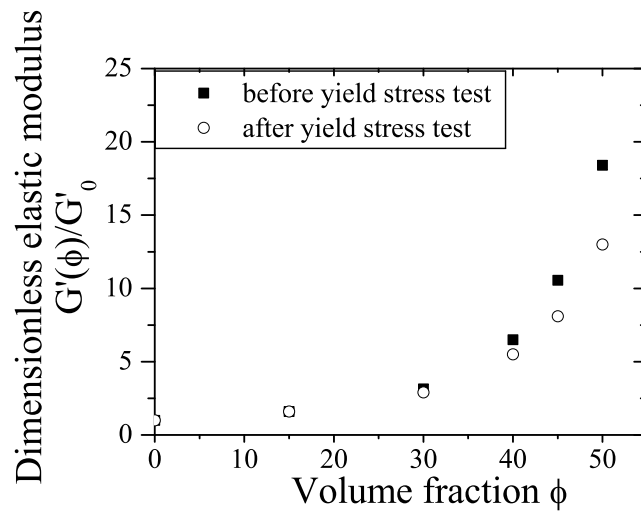


Figure 12: Dimensionless elastic modulus $G'(\phi)/G'(0)$ vs. the beads volume fraction ϕ for suspensions of 2mm glass beads in a Carbopol gel before (filled squares) and after (open circles) the yield stress measurements.

We observe in Fig. 12 that the material was changed by the slow shear: it appears to be less stiff after the shear than before the yield stress measurement. The change can be rather important as the dimensionless modulus measured before the slow shear is 40% higher than the

modulus measured after the slow shear in the case of the 50% suspension.

Let us now examine the possible reasons for this change. First, one should notice that as both measurements ($G'(\phi)$ and $G'(0)$) are performed in the same conditions, the difference in the $G'(\phi)/G'(0)$ values cannot be attributed to the small rejuvenation of the suspending fluid by the shear, which should be roughly the same with and without beads (note moreover from Fig. 1 that the possible variation of the elastic modulus of the Carbopol gel due to shear is of order 5%).

A possibility, as pointed out in Sec. II is that shear-induced migration of the particles has begun to occur as such a phenomenon would lead to an apparent decrease in the elastic modulus. However, it should be noted that one would not expect a deformation of 3 to generate significant migration; nevertheless, at such low velocity the flow is likely to be localized near the inner cylinder and it is still possible that the depletion of particles near the inner tool is thus a rapid phenomenon that leads to a decrease in the apparent elastic modulus.

Another possibility is that the suspension microstructure has become anisotropic: it is known that under shear suspensions of particles develop an anisotropic microstructure [Parsi and Gadala-Maria (1987); Morris and Brady (1996)]. It has been shown by Gadala-Maria and Acrivos (1980), Narumi et al. (2002) and Narumi et al. (2005) that the stationary anisotropic structure is reached for a deformation of order 2. It is thus highly probable that the decrease in the elastic modulus we observe at high concentrations is a signature of the development of a particle anisotropy due to shear.

To conclude, since we want to deal with homogeneous and isotropic materials, only the first elasticity and yield stress measurements can be trusted. Any other measurement requires a new preparation of the material.

V Elastic modulus vs. yield stress: comparison with a micromechanical approach

Proposing a theoretical value for the dimensionless elastic modulus and the dimensionless yield stress is challenging; e.g., in a micromechanical approach, the final result depends on the scheme that is chosen. However, it is shown in a companion paper by Chateau *et al.* (2007) that it is possible to give a general relationship between the linear response of the materials (e.g. its dimensionless elastic modulus $G'(\phi)/G'(0)$ as in our study) and the dimensionless yield stress $\tau_c(\phi)/\tau_c(0)$ of a suspension of rigid particles in a yield stress fluid that is true whatever the scheme (the way the phases interact one with the other) as long as the particle distribution is isotropic, and provided the strain heterogeneities are weak (i.e. this should not be true at high volume fractions; this last point is discussed in detail by Chateau *et al.* (2007)).

Chateau *et al.* (2007) find

$$\frac{\tau_c(\phi)}{\tau_c(0)} = \sqrt{(1 - \phi) \frac{G'(\phi)}{G'(0)}} \quad (4)$$

Note that the micromechanical estimate of Chateau *et al.* (2007) is based on the following hypotheses: the particles are rigid, monodisperse and noncolloidal; there are no physicochemical interactions between the particles and the paste; the distribution of the particles is isotropic. This is what we have managed to perform experimentally, therefore, our experiments are fitted to provide a test of these theoretical predictions.

In Fig. 13, we plot the dimensionless yield stress $\tau_c(\phi)/\tau_c(0)$ vs. a function of the dimensionless elastic modulus $\sqrt{(1 - \phi)G'(\phi)/G'(0)}$ for all the systems studied in logarithmic coordinates.

We observe a remarkable agreement between our results and the micromechanical estimation of Eq. 4 (that is plotted as a straight line $y = x$ in these coordinates). As a consequence,

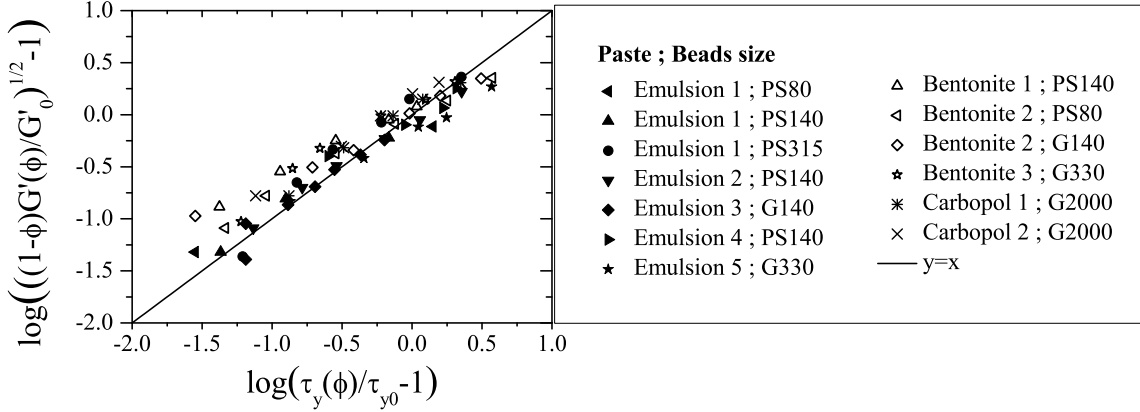


Figure 13: Dimensionless yield stress $\log(\tau_c(\phi)/\tau_c(0) - 1)$ vs. some function of the dimensionless elastic modulus $\log(\sqrt{(1-\phi)G'(\phi)/G'(0)} - 1)$ for all the systems studied. The line is a $y = x$ plot corresponding to the theoretical prediction of Chateau *et al.* (2007).

combining Eq. 2 and Eq. 4, this yields for the yield stress

$$\frac{\tau_c(\phi)}{\tau_c(0)} = \sqrt{\frac{1-\phi}{(1-\phi/\phi_m)^{2.5\phi_m}}} \quad (5)$$

with $\phi_m = 0.57$, which is plotted in Fig. 11, and of course is well fitted to the experimental data.

Eq. 4 also means that the critical yield strain γ_c , defined as the strain at which a flow starts, follows a law

$$\gamma_c(\phi) \approx \frac{\tau_c(\phi)}{G'(\phi)} = \gamma_c(0) \sqrt{(1-\phi)G'(0)/G'(\phi)} \quad (6)$$

which, together with Eq. 2 yields

$$\gamma_c(\phi) = \gamma_c(0) \sqrt{(1-\phi)(1-\phi/\phi_m)^{2.5\phi_m}} \quad (7)$$

From Eq. 4, we see that measuring the linear properties of suspensions helps to find the non-linear properties of suspensions in yield stress fluids; theoretically, this linear response could be measured as the viscosity of suspensions of noncolloidal particles in Newtonian fluids. However,

it should be noted that usually the viscosity measurements of suspensions are performed on an anisotropic structure induced by the flow [Parsi and Gadala-Maria (1987)]. As a consequence, most viscosity laws one can find in the literature cannot be used to predict the yield stress of isotropic suspensions of noncolloidal particles in yield stress fluids, whereas our elasticity measurements can.

Finally, note that Eq. 4 is very different from what can be observed in colloidal suspension in which the elastic modulus and the yield stress follow roughly the same evolution with the volume fraction ψ of colloidal particles (see Appendix B for an example).

VI Conclusion

We have studied experimentally the behavior of isotropic suspensions of monodisperse rigid spherical noncolloidal particles in yield stress fluids. In order to evaluate the purely mechanical contribution of the particles to the paste behavior, independently of the physicochemical properties of the materials, we have suspended beads of various sizes, made of various materials in very different pastes (an emulsion, a microgel, and a colloidal suspension) whose common point is to exhibit a yield stress, and we sought consistency between the results. We focused on the influence of the particles on the elastic modulus and the yield stress; we used experimental procedures designed to ensure isotropy of the suspensions. We showed that the dimensionless elastic modulus $G'(\phi)/G'(0)$ and the dimensionless yield stress $\tau_c(\phi)/\tau_c(0)$ depend on the bead volume fraction ϕ only. We found that the elastic modulus/concentration relationship is well fitted to a Krieger-Dougherty law $(1 - \phi/\phi_m)^{-2.5\phi_m}$ with $\phi_m = 0.57$, and showed that the yield stress/concentration relationship is related to the elastic modulus/concentration relationship through a very simple law $\tau_c(\phi)/\tau_c(0) = \sqrt{(1 - \phi)G'(\phi)/G'(0)}$, in agreement with recent results from a micromechanical analysis. We now plan to study the case of bidisperse systems and of anisotropic particle distributions. We also intend to study the influence of the particle on the flow behavior and the phenomenon of particle migration through MRI techniques.

Appendix A: Nonmechanical effects

In this appendix, we present how physicochemical interactions between some particles and some pastes can be evidenced: first, thanks to the measurement of the temporal evolution of the elastic modulus, second, thanks to the experiments performed with various bead sizes. This allows eliminating unambiguously some materials from the analysis. This shows that all the points we raised in Sec. II should be checked carefully when embedding particles in a yield stress fluid if one wants to deal with the general problem of any rigid particle in any yield stress fluid.

Physicochemical effects in the emulsion and the bentonite suspension

As mentioned in Sec. III, a condition necessary to fulfill if there are no physicochemical interactions between the beads and the yield stress fluid is that the dimensionless elastic modulus $G'(\phi, t)/G'(0, t)$ does not depend on time, whatever the volume fraction ϕ is. This condition was fulfilled on the data presented on Fig. 6.

In a few cases, we found however that it would depend on time. In the case of the bentonite suspension, one can still argue that our procedure does not allow to get a reproducible initial state, and that may cause $G'(\phi, t)/G'(0, t)$ to evolve in time as the interstitial paste in the suspension is not the same as the pure paste. In the case of the emulsion, the pure emulsion modulus does not depend on time. Therefore, even if the manual preparation does not allow to get a perfectly reproducible interstitial paste as mentioned in Sec.II, this paste properties should not evolve in time when beads are embedded into it. Fig. 14 shows the elastic modulus evolution in time of an emulsion and of the same emulsion filled with $140\mu\text{m}$ PS beads.

In Fig. 14 we observe that the pure emulsion modulus is constant in time, whereas the 30% suspension modulus evolves in time; there is no reason why it should evolve, therefore we have to conclude that the emulsion studied in Fig. 14 was somehow modified by the inclusion of beads. Note that this behavior was observed only in 2 emulsions, with 80 and $140\mu\text{m}$ PS beads (even if carefully washed). We did not correlate this behavior with a particular formulation.

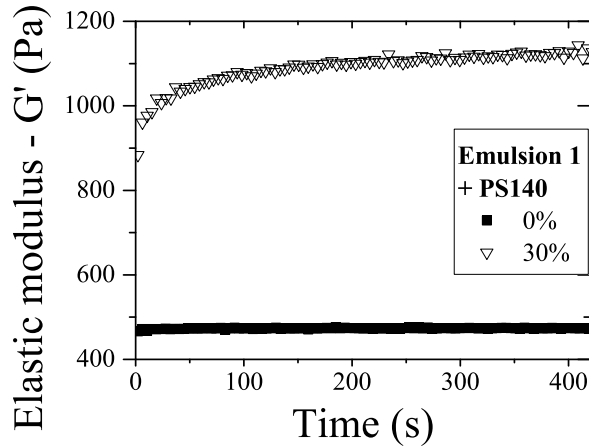


Figure 14: Elastic modulus vs. time for a pure emulsion and for the same emulsion filled with 30% of $140\mu\text{m}$ PS beads.

All the materials exhibiting this behavior were eliminated from our analysis as they did not fulfill our aim of having purely mechanical interactions.

More generally, looking at the dimensionless modulus as a function of time thus seems a good test to study any suspension of particles in a yield stress fluid if one seeks a general result (i.e. not specific to the materials studied).

Size effects in Carbopol gels

As mentioned in Sec. III, a condition necessary to fulfill if there are no physicochemical interactions between the beads and the yield stress fluid is that the dimensionless elastic modulus $G'(\phi)/G'(0)$ does not depend on the bead size. This condition was fulfilled on the data presented on Fig. 8.

In Fig. 15, we plot the dimensionless elastic modulus $G'(\phi)/G'(0)$ vs. the beads volume fraction ϕ for suspensions of $80\mu\text{m}$, $140\mu\text{m}$, and 2mm polystyrene and glass beads in a Carbopol gel.

We observe that in this material only, the evolution of the dimensionless elastic modulus with the volume fraction depends on the bead size and material. In the case of the $80\mu\text{m}$ and $140\mu\text{m}$

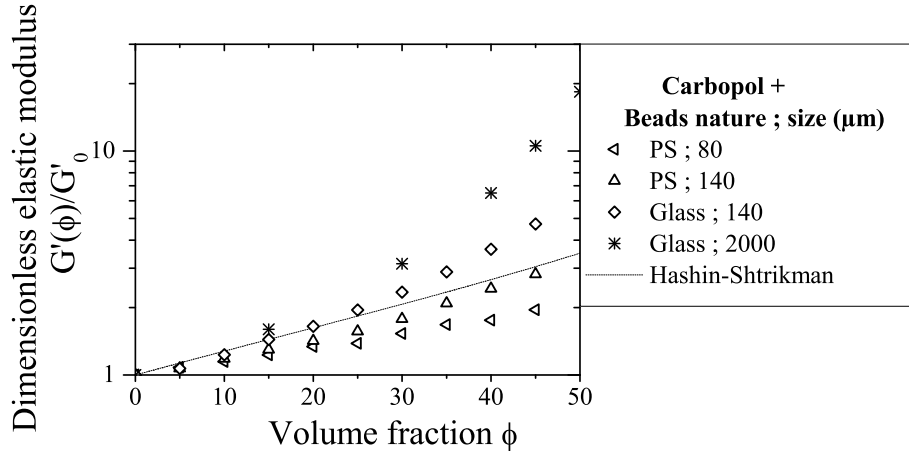


Figure 15: Dimensionless elastic modulus $G'(\phi)/G'(0)$ vs. the beads volume fraction ϕ for suspensions of $80\mu\text{m}$, $140\mu\text{m}$, and 2mm polystyrene and glass beads in a Carbopol gel. The line is the Hashin-Shtrikman bound $(2 + 3\phi)/(2 - 2\phi)$.

PS beads, the data fall below the Hashin-Shtrikman bound: this means that the conditions are not fulfilled for correct homogenization in these cases. On the other hand, as expected, our data with the 2mm beads are consistent with all the results obtained on the emulsion and the bentonite suspension, whatever the bead size. This may be due to two problems: (i) the Carbopol may be extremely sensitive to surface physicochemical interactions; (ii) the microstructure size may be of the order of several tens of μm (as mentioned in the introduction, the Carbopol gel microstructure is actually poorly known and there is only indirect evidence that the microstructure size may be of the order of a few microns). In both cases, we expect the effect of the size to disappear when the bead size is increased.

This problem, together with the structuration of Carbopol gels under shear (see the end of Sec. II), point out the fact that Carbopol gels are probably not the ideal model yield stress fluids. It is important to note that this complexity exists as Carbopol gels are often used as model yield stress fluids. We think that an emulsion is more fitted to play this role.

Appendix B: Comparison with colloidal suspensions

In order to see if the features we observe, and particularly Eq. 4, are special features of non-colloidal suspensions embedded in a colloidal paste, we have qualitatively studied the evolution of the yield stress and the elastic modulus of a colloidal paste with the volume fraction of its colloidal particles. We prepared bentonite suspensions of volume fraction ψ ranging between 3 and 9%, and measured the evolution with time and concentration of their elastic modulus $G'(\psi, t)$ and yield stress $\tau_c(\psi, t)$ with the procedures defined in Sec. II.

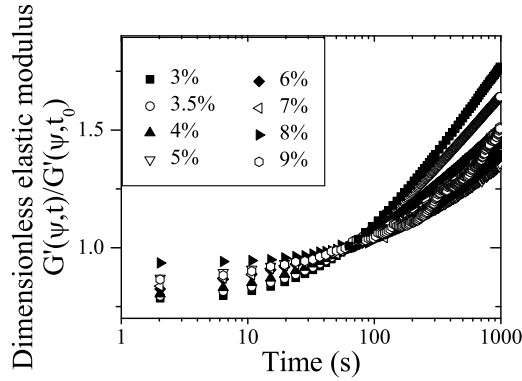


Figure 16: a) Dimensionless elastic modulus $G'(\psi, t)/G'(\psi, t_0 = 60s)$ vs. time for bentonite suspensions at bentonite particles volume fraction ranging between 3 and 9%.

A first striking difference between both systems is that it is difficult to study the evolution of the elastic modulus or the yield stress of thixotropic materials with the volume fraction, because the kinetics of their evolution depends on the volume fraction of colloidal particles: when plotted vs. time, $G'(\psi, t)/G'(\psi, t_0 = 60s)$ does not yield a unique time-dependent function but depends on the concentration (see Fig. 16). While the structuration kinetics of a given thixotropic material does not depend on the noncolloidal particles added into it (see Sec.III), it depends a lot on the concentration of colloidal particles.

At a first glance, it thus seems difficult to analyze the colloidal particles case. It has been shown however by Ovarlez and Coussot (2007) that it is possible to distinguish between the

influence of ψ on the elastic modulus evolution (which is what we are searching) and on the structuration kinetics. It is out of the scope of this paper to go further on this particular point, and at this stage we consider that computing the dimensionless elastic modulus and yield stress at a given time provides nevertheless a rather good evaluation of the colloidal particle concentration ψ influence on the mechanical properties of the colloidal paste.

In Fig. 17 we plot the dimensionless elastic modulus $G'(\psi, t)/G'(\psi_0 = 3\%, t)$ and yield stress $\tau_c(\psi, t)/\tau_c(\psi_0 = 3\%, t)$ computed at several rest times t vs. the colloidal particle volume fraction ψ .

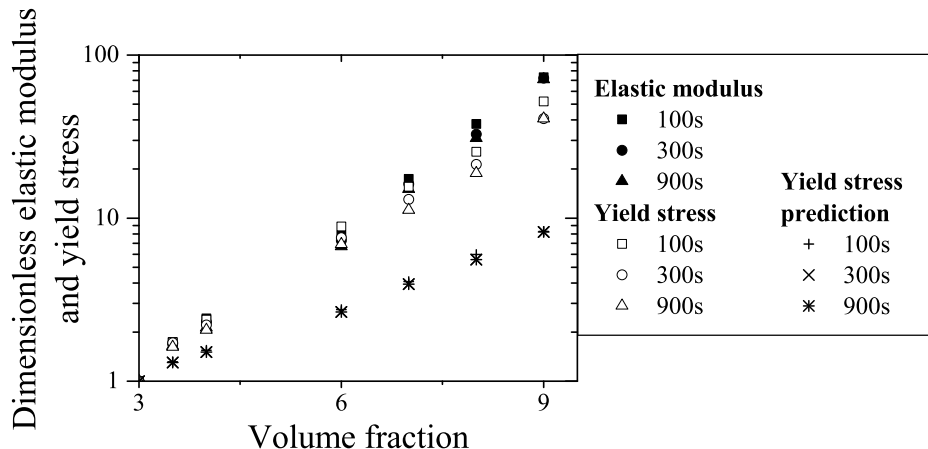


Figure 17: Dimensionless elastic modulus $G'(\psi, t)/G'(\psi_0 = 3\%, t)$ (filled symbols) and yield stress $\tau_c(\psi, t)/\tau_c(\psi_0 = 3\%, t)$ (open symbols) computed at a rest time $t = 100, 300$ and 900 s, vs. the colloidal particle volume fraction ψ , for bentonite suspensions of bentonite particle volume fraction ranging between 3 and 9% . The crosses are the dimensionless yield stress predictions from Eq. 4.

In contrast with what was observed when noncolloidal particles are added into the paste (Sec. III and Sec. IV), we observe that the yield stress and elastic modulus evolution with ψ are roughly identical. In order to compare these results with the noncolloidal case, we also plot in Fig. 17 the predictions for the yield stress given by Eq. 4 as a function of the elastic modulus

values: in the coordinates of Fig. 17, this would yield:

$$\frac{\tau_{c,model}(\psi)}{\tau_{c,model}(\psi_0 = 3\%)} = \sqrt{\frac{(1 - \psi)G'(\psi)}{(1 - 0.03)G'(\psi_0 = 3\%)}} \quad (8)$$

We find that the model describing the influence of noncolloidal particles would predict a much lower increase of the yield stress.

To conclude, the evolution of the behavior of suspensions of noncolloidal particles in yield stress fluids with the noncolloidal particle volume fraction ϕ is very different from the evolution of the properties of a colloidal paste when increasing the colloidal particle volume fraction ψ . The colloidal paste structuration kinetics depends on ψ (whereas it does not depend on ϕ), and its yield stress τ_c follows the same rapid evolution with ψ than its elastic modulus G' (whereas τ_c increases much less rapidly with ϕ than G' , see Eq. 4).

References

- Abbott, J. R., N. Tetlow, A. L. Graham, S. A. Altobelli, E. Fukushima, L. A. Mondy, and T. S. Stephens, "Experimental observations of particle migration in concentrated suspensions: Couette flow," *J. Rheol.* **35**, 773-795 (1991).
- Ancey, C., and H. Jorrot, "Yield stress for particle suspensions within a clay dispersion," *J. Rheol.* **45**, 297-319 (2001).
- Brady, J. F., and J. F. Morris, "Microstructure of strongly sheared suspensions and its impact on rheology and diffusion," *J. Fluid Mech.* **348**, 103-139 (1997).
- Carnali, J. O., and M. S. Naser, "The use of dilute suspension viscosimetry to characterize the network properties of Carbopol microgels," *Colloid Polym. Sci.* **270**, 183-193 (1992).
- Chateau, X., G. Ovarlez, and K. Luu Trung, "Homogenization approach to the behavior of sus-

- pensions of noncolloidal particles in yield stress fluids,” submitted to the Journal of Rheology (2007).
- Cheng, D. C. H. “Yield stress: A time-dependent property and how to measure it,” *Rheol. Acta*, **25**, 542-554 (1986).
- Cohen-Addad, S., M. Krzan, R. Höhler, and B. Herzhaft, “Rigidity percolation in particle laden foams,” *Phys. Rev. Lett.* **99**, 168001 (2007).
- Coussot, P., and S. Boyer, “Determination of yield stress fluid behaviour from inclined plane test,” *Rheol. Acta* **34**, 534-543 (1995).
- Coussot, P., *Mudflow Rheology and Dynamics* (Balkema, Rotterdam, 1997).
- Coussot, P., *Rheometry of Pastes, Suspensions and Granular Materials* (John Wiley & Sons, New York, 2005).
- Coussot, P., H. Tabuteau, X. Chateau, L. Tocquer, and G. Ovarlez, “Aging and solid or liquid behavior in pastes,” *J. Rheol.* **50**, 975-994 (2006).
- Gadala-Maria, F., and A. Acrivos, “Shear-induced structure in a concentrated suspension of solid spheres,” *J. Rheol.* **24**, 799-814 (1980).
- Geiker M. A., M. Brandl, L. Thrane, N. F. Nielsen, “On the Effect of Coarse Aggregate Fraction and Shape on the Rheological Properties of Self-Compacting Concrete,” *Cement, Concrete, and Aggregates* **24**, 3-6 (2002).
- Graham, A. L., S. A. Altobelli, E. Fukushima, L. A. Mondy, and T. S. Stephens, “Note: NMR imaging of shear-induced diffusion and structure in concentrated suspensions undergoing Couette flow,” *J. Rheol.* **35**, 191-201 (1991).
- Hashin, Z., and S. Shtrikman, “A variational approach to the theory of the elastic behaviour of multiphase materials”, *J. Mech. Phys. Solids.* **11**, 127-140 (1963).

- Huang, P. Y., and D. D. Joseph, "Effects of shear thinning on migration of neutrally buoyant particles in pressure driven flow of Newtonian and viscoelastic fluids," *J. Non-Newtonian Fluid Mech.* **90**, 159-185 (2000).
- Ketz, R. J., R. K. Prud'homme, and W. W. Graessley, "Rheology of concentrated microgel solutions," *Rheol. Acta* **27**, 531-539 (1988).
- Kim, J.-Y., J.-Y. Song, E.-J. Lee, and S.-K. Park, "Rheological properties and microstructures of Carbopol gel network system," *Colloid Polym. Sci.* **281**, 614-623 (2003).
- Krieger, I. M., and T. J. Dougherty, "A Mechanism for Non-Newtonian Flow in Suspensions of Rigid Spheres," *J. Rheol.* **3**, 137-152 (1959).
- Larson, R. G., *The structure and rheology of complex fluids* (Oxford University Press, New York, 1999).
- Leighton, D., and A. Acrivos, "The shear-induced migration of particles in concentrated suspensions," *J. Fluid Mech.* **181**, 415-439 (1987b).
- Liddell, P. V., and D.V. Boger, "Yield stress measurements with the vane," *J. Non-Newtonian Fluid Mech.* **63**, 235-261 (1996).
- Lormand, B. M., and R. J. Phillips, "Sphere migration in oscillatory Couette flow of a viscoelastic fluid," *J. Rheol.* **48**, 551-570 (2004).
- Mills, P., and P. Snabre, "Rheology and Structure of Concentrated Suspensions of Hard Spheres. Shear Induced Particle Migration," *J. Phys. II France* **5**, 1597-1608 (1995).
- Morris, J. F., and J. F. Brady, "Self-diffusion in sheared suspensions," *J. Fluid Mech.* **312**, 223-252 (1996).
- Morris, J. F., and F. Boulay, "Curvilinear flows of noncolloidal suspensions: The role of normal stresses," *J. Rheol.* **43**, 1213-1237 (1999).

- Narumi, T., H. See, Y. Honma, T. Hasegawa, T. Takahashi, and N. Phan-Thien, "Transient response of concentrated suspensions after shear reversal," *J. Rheol.* **46**, 295305 (2002).
- Narumi, T., H. See, A. Suzuki, and T. Hasegawa, "Response of concentrated suspensions under large amplitude oscillatory shear flow," *J. Rheol.* **49**, 7185 (2005).
- Nguyen, Q. D., and D. V. Boger, "Direct yield stress measurement with the vane method," *J. Rheol.* **29**, 335-347 (1985).
- Nott, P., and J. F. Brady, "Pressure-driven flow of suspensions: Simulation and theory," *J. Fluid Mech.* **275**, 157-199 (1994).
- Oppong, F. K., L. Rubatat, B. J. Frisken, A. E. Bailey, and J. R. de Bruyn, "Microrheology and structure of a yield-stress polymer gel," *Phys. Rev. E* **73**, 041405 (2006).
- Ovarlez, G., F. Bertrand, and S. Rodts, "Local determination of the constitutive law of a dense suspension of noncolloidal particles through magnetic resonance imaging," *J. Rheol.* **50**, 259-292 (2006).
- Ovarlez, G., and P. Coussot, "The physical age of soft-jammed systems," to appear in *Physical Review E* (2007).
- Parsi, F., and F. Gadala-Maria, "Fore-and-aft asymmetry in a concentrated suspension of solid spheres," *J. Rheol.* **31**, 725-732 (1987).
- Pashias, N. D. V. Boger, J. Summers, and D. J. Glenister, "A fifty cent rheometer for yield stress measurement," *J. Rheol.* **40**, 1179-1189 (1996).
- Phillips, R. J., R. C. Armstrong, R. A. Brown, A. L. Graham, and J. R. Abbott, "A constitutive equation for concentrated suspensions that accounts for shear-induced particle migration," *Phys. Fluids* **4**, 30-40 (1992).

- Poslinski, A. J., M. E. Ryan, R. K. Gupta, S. G. Seshadri, and F. J. Frechette, "Rheological Behavior of Filled Polymeric Systems I. Yield Stress and Shear-Thinning Effects," *J. Rheol.* **32**, 703-735 (1988).
- Roussel, N., and P. Coussot "Fifty-cent rheometer for yield stress measurements: From slump to spreading flow," *J. Rheol.* **49**, 705-718 (2005).
- See, H., P. Jiang, and N. Phan-Thien, "Concentration dependence of the linear viscoelastic properties of particle suspensions," *Rheol. Acta*, **39**, 131-137 (2000).
- Sengun, M. Z. and R. F. Probstein, "Bimodal model of slurry viscosity with application to coal-slurries. Part 1. Theory and experiment," *Rheol. Acta* **28** 382-393 (1989).
- Sengun, M. Z. and R. F. Probstein, "Bimodal model of slurry viscosity with application to coal-slurries. Part 2. High shear limit behavior," *Rheol. Acta* **28** 394-401 (1989).
- Shapley, N. C., R. A. Brown, and R. C. Armstrong, "Evaluation of particle migration models based on laser Doppler velocimetry measurements in concentrated suspensions," *J. Rheol.* **48**, 255-279 (2004).
- Sierou, A., and J. F. Brady, "Rheology and microstructure in concentrated noncolloidal suspensions," *J. Rheol.* **46**, 1031-1056 (2002).
- Stickel, J. J., and R. L. Powell, "Fluid Mechanics and Rheology of Dense Suspensions," *Annu. Rev. Fluid Mech.* **37**, 129-149 (2005).
- Tehrani, M. A., "An experimental study of particle migration in pipe flow of viscoelastic fluids," *J. Rheol.* **40**, 1057-1077 (1996).
- Uhlerr, P. H. T., J. Guo, C. Tiu, X. M. Zhang, J. Z. Q. Zhou, and T. N. Fang, "The shear-induced solid-liquid transition in yield stress materials with chemically different structures," *J. Non-Newtonian Fluid Mech.* **125**, 101-119 (2005).

Walberer, J. A., and A. J. McHugh, “The linear viscoelastic behavior of highly filled polydimethylsiloxane measured in shear and compression”, *J. Rheol.* **45**, 187-201 (2001).

Zarraga, I. E., D. A. Hill, and D. T. Leighton, “The characterization of the total stress of concentrated suspensions of noncolloidal spheres in Newtonian fluids” *J. Rheol.* **44**, 185-220 (2000).